# Exceptional Points of Degeneracy in Electromagnetic Periodic Waveguides and the Role of Symmetries

Tarek Mealy, Mohamed Y. Nada, Ahmed F. Abdelshafy, Ehsan Hafezi, and Filippo Capolino

Department of Electrical Engineering and Computer Science, University of California, Irvine, CA 92697, USA, email: f.capolino@uci.edu

Abstract— We investigate the role of reflection and glide symmetry in periodic lossless waveguides on the dispersion diagram and on the existence of various orders of exceptional points of degeneracy (EPDs). We use an equivalent circuit network to model each unit-cell of the guiding structure. Assuming that a coupled-mode waveguide supports N modes in each direction, we derive the following conclusions. When N is even, we show that a periodic guiding structure with reflection symmetry may exhibit EPDs of maximum order N. To obtain a degenerate band edge (DBE) with only two coupled guiding structures, reflection symmetry must be broken. For odd N, N+1 is the maximum EPD order that may be obtained, and an EPD of order N is not allowed. We present an example of three coupled microstrip transmission lines and show that breaking the reflection symmetry by introducing glide symmetry enables the occurrence of a stationary inflection point (SIP), also called frozen mode, which is an EPD of order three.

*Index Terms*—Periodic structures, degeneracy, glide symmetry.

## I. INTRODUCTION

Exceptional points of degeneracy (EPDs) are points in an electromagnetic system parameters space where two or more eigenmodes coalesce into a single eigenmode. The dispersion relation of eigenmodes in a waveguide that exhibits an EPD with order m, where m is the number of coalescing eigenmodes, has the behavior of  $(\omega - \omega_e) \propto (k - k_e)^m$  at the vicinity of an EPD  $(\omega_e, k_e)$  [1]-[2]. Here  $\omega$  and k are the angular frequency and the wavenumber, respectively, and the EPD is denoted by the subscript e. Such dispersion behavior is accompanied by a severe reduction in the group velocity of waves propagating in those structures resulting in a giant increase in the loaded quality factor and the local density of states which is beneficial for various applications such as pulse generators and compressors, high-Q resonators, sensors and lasers.

The simplest second order EPD is found in uniform waveguides at the modal cutoff frequency [3]. Second order EPDs in the form of band edges also occur in lossless periodic waveguides; they are also realized in uniform coupled transmission lines (CTLs) by introducing parity-time (PT-) symmetry [4]-[5] which implies using a balanced and symmetrical distribution of gain and loss [6]. Different orders of EPD, especially the degenerate band edge (DBE) which is an EPD of order four, have been engineered in various types of periodic guided structures in [7]-[11]. Waveguides

supporting a stationary inflection point (SIP), which is an EPD of order 3, are shown in [12]-[13]. In [11], some of the authors have shown the relation between gain and loss balance condition for the existence of EPD in two coupled guiding structures. Also, in [11] the DBE was experimentally demonstrated in two coupled microstrip lines. Compared to the work presented in [11], here we consider guiding structures that are lossless and gainless, and we focus only on the role of symmetry in coupled waveguides to exhibit EPDs, in particular a DBE or an SIP.

The existence of symmetry in periodic waveguides plays an important role in the kind of modes that are allowed and the maximum order of EPD that can be obtained. In this paper, we study the relation between reflection and glide symmetry in coupled waveguides and the orders of EPDs that can be obtained in such electromagnetic systems.

A periodic waveguide is said to possess a higher symmetry if it consists of more than a simple translation or reflection symmetry [14]. A periodic waveguide is said to possess a glide symmetry if it remains invariant under the glide operation G, consisting of a translation by half of the geometrical period d, followed by a reflection in the so-called glide plane [15]-[16]. The experimental verification of an SIP in a three-way microstrip waveguide with glide symmetry was presented in [17].

In this paper, we focus on the role that the symmetry in periodic coupled waveguides have in establishing an EPD. We show that reflection symmetry in guiding structures enforces a maximum limit to the order of the EPD that is obtainable. Additionally, we present an example showing that breaking reflection symmetry by introducing higher symmetry, e.g., glide symmetry, enables the existence of EPD of special order that cannot be obtained in electromagnetic structures that have reflection symmetry. The EPD we consider in this paper are shown for guiding structures that are lossless and gainless; hence they are the regular band edge (an EPD of order 2), the DBE and the SIP.

#### II. SYSTEM MODELING

Figures 1(a) and 1(b) show two arbitrary periodic structures with reflection (mirror) symmetry and glide symmetry, respectively. The type of symmetry is determined by the operator under which the fields are invariant.

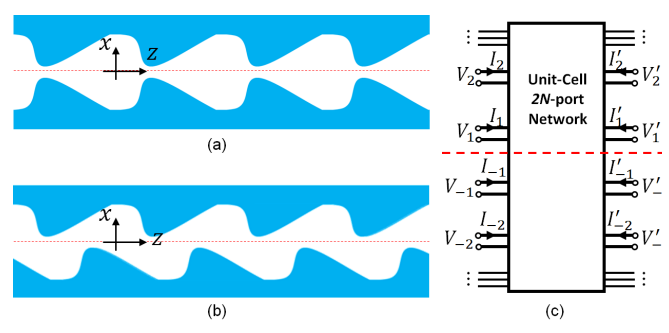


Fig. 1. (a) An arbitrary shape periodic structure with reflection (mirror) symmetry. The blue color represents either metal or dielectric. The structure may be 2D or 3D. (b) Waveguide with glide symmetry. (c) A multimodal circuit network model for a 2*N*-port unit cell of either (a) or (b).

The reflection (mirror) symmetry operator  $R_{\hat{x}}$  and glide symmetry operator  $G_{\hat{x}}$  apply to the fields and are defined as follows

$$R_{\hat{x}}: (x,z) \to (-x,z),$$

$$G_{\hat{y}}: (x,z) \to (-x,z+d/2).$$
(1)

When the reflection symmetry operator applies to electromagnetic fields, it results in mirroring the fields around the plane of symmetry (red dashed line in Fig. 1(a)). On the other hand, applying the glide symmetry operator to fields in periodic waveguides results in a translation of the fields by half a period and then mirroring them around the plane of symmetry.

Waves in the periodic guiding structure shown in Figs. 1(a) and (b) are represented by ports at the start and the end of each unit cell. An equivalent 2N-port network is shown in Fig. 1(c), where N is the number of modes at each side of the network, i.e., N is the number of the coupled waveguides in the guided electromagnetic structure. For example, the waveguides in Fig. 2 and Fig. 3 have N=4 and N=3, respectively, and they are also called 4-way and 3-way coupled waveguides.

We consider two cases, in the first case N is *even* and in the second one N is *odd*. Let us consider first the case where N is even, represented by the periodically coupled waveguides based on four microstrip lines above a grounded dielectric substrate whose unit cell is shown in Fig. 2.

For convenience, we define a state vector  $\Psi = \left[ \Psi_U^T, \ \Psi_L^T \right]^T$  that describes the electromagnetic fields at any coordinate z, where the subscript U and L are designated for the upper and lower state vectors, respectively,  $\Psi_U$  and  $\Psi_L$ , and the superscript T denotes the transpose operation. They represent the state vectors associated to voltages and currents in the upper and lower half spaces, respectively, referring to Fig. 2. They are defined as

$$\mathbf{\Psi}_{U} = \begin{bmatrix} \mathbf{\Psi}_{1}^{T}, & \mathbf{\Psi}_{2}^{T}, & \dots & \mathbf{\Psi}_{N/2}^{T} \end{bmatrix}^{T},$$

$$\mathbf{\Psi}_{L} = \begin{bmatrix} \mathbf{\Psi}_{-1}^{T}, & \mathbf{\Psi}_{-2}^{T}, & \dots & \mathbf{\Psi}_{-N/2}^{T} \end{bmatrix}^{T},$$
(2)

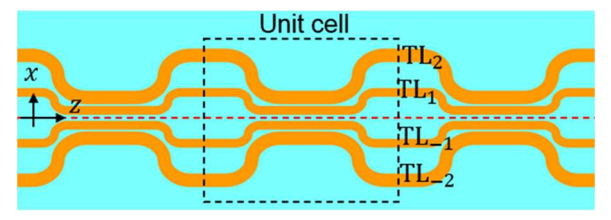


Fig. 2. Example of four periodically coupled microstrip transmission lines above a grounded dielectric substrate, with reflection (mirror) symmetry.

where N here is the total number of modes used to model fields. Each  $\Psi_n$  in (2), with  $n=\pm 1,\pm 2,\pm 3,...$  is a vector of the transmission line voltage and current, as also discussed in [11]. Note that the negative sign for state vector indices represents modes in the lower half space, i.e. x<0, while the positive one represents modes in the upper half space. Based on the equivalent circuit network shown in Fig. 1(c), the relation between the input state vector  $\Psi(z)$  and the output state vector  $\Psi(z+d)$  of a given unit-cell is defined by the transfer matrix  $\underline{\mathbf{T}}(z)$ , such as  $\Psi(z+d) = \underline{\mathbf{T}}(z)\Psi(z)$ , which is written in block matrix form as

$$\begin{bmatrix} \mathbf{\Psi}_{U}(z+d) \\ \mathbf{\Psi}_{L}(z+d) \end{bmatrix} = \begin{bmatrix} \mathbf{T}_{UU}(z) & \mathbf{T}_{UL}(z) \\ \mathbf{T}_{UL}(z) & \mathbf{T}_{UL}(z) \end{bmatrix} \begin{bmatrix} \mathbf{\Psi}_{U}(z) \\ \mathbf{\Psi}_{L}(z) \end{bmatrix}$$
(3)

Applying operators (1) to any electromagnetic state  $\Psi(z)$ , we get

$$R_{\hat{x}} : \Psi(z) \to \underline{\mathbf{R}}\Psi(z),$$

$$G_{\hat{x}} : \Psi(z) \to \mathbf{T}_{1/2}(z)\mathbf{R}\Psi(z),$$
(4)

where  $\mathbf{R}$  is the  $2N \times 2N$  mirror symmetry matrix

$$\underline{\mathbf{R}} = \begin{bmatrix} \mathbf{0} & \underline{\mathbf{I}} \\ \underline{\mathbf{I}} & \mathbf{0} \end{bmatrix}, \tag{5}$$

 $\underline{\underline{I}}$  is the  $N \times N$  identity matrix, and  $\underline{\mathbf{T}}_{1/2}(z)$  is the  $2N \times 2N$  transmission matrix of half period calculated at position z, i.e.,  $\underline{\Psi}(z+d/2) = \underline{\mathbf{T}}_{1/2}(z)\underline{\Psi}(z)$ . We recall that the state vector  $\underline{\Psi}(z)$  is made of 2N components, since each  $\underline{\Psi}_n$  has dimension 2.

Waveguides with symmetries as in Fig. 1 are better understood by using an even and odd mode representation. Hence, we define a new state vector

$$\mathbf{X} = \left[ \left( \mathbf{\Psi}_{U} + \mathbf{\Psi}_{L} \right)^{T}, \quad \left( \mathbf{\Psi}_{U} - \mathbf{\Psi}_{L} \right)^{T} \right]^{T} = \underline{\mathbf{t}} \, \mathbf{\Psi}, \text{ where}$$

$$\underline{\mathbf{t}} = 2\underline{\mathbf{t}}^{-1} = \underline{\mathbf{R}} + \underline{\mathbf{I}}, \text{ and } \underline{\mathbf{I}} \text{ is}$$

$$\underline{\mathbf{I}} = \begin{bmatrix} \underline{\mathbf{I}} & \mathbf{0} \\ \underline{\mathbf{0}} & -\underline{\mathbf{I}} \end{bmatrix}. \tag{6}$$

By applying this basis transformation to (3), we obtain  $\mathbf{X}(z+d) = \underline{\mathbf{t}} \underline{\mathbf{T}} \underline{\mathbf{t}}^{-1} \mathbf{X}(z) = \underline{\mathbf{T}}_X \mathbf{X}(z)$  where the transfer matrix  $\underline{\mathbf{T}}_X$  is given by

$$\underline{\mathbf{T}}_{X} = \begin{bmatrix} \mathbf{T}_{UU}(z) + \mathbf{T}_{UL}(z) & \mathbf{0} \\ \mathbf{0} & \mathbf{T}_{LL}(z) - \mathbf{T}_{LU}(z) \end{bmatrix} + 0.5(\mathbf{RTR} - \mathbf{T})(\mathbf{I} + \mathbf{RI}').$$
(7)

For guiding structures with reflection symmetry, we know that  $\underline{\mathbf{T}}_{UU}(z) = \underline{\mathbf{T}}_{LL}(z)$  and  $\underline{\mathbf{T}}_{UL}(z) = \underline{\mathbf{T}}_{LU}(z)$ . This implies that  $\underline{\mathbf{R}}$  and  $\underline{\mathbf{T}}$  commute, i.e.,  $\underline{\mathbf{R}}\underline{\mathbf{T}} = \underline{\mathbf{T}}\underline{\mathbf{R}}$ , consequently  $\underline{\mathbf{M}}\underline{\mathbf{T}}\underline{\mathbf{M}} - \underline{\mathbf{T}} = \underline{\mathbf{0}}$  which means that  $\underline{\mathbf{T}}_X$  in (7) is a block diagonal matrix. Therefore, we do not have coupling between even and odd modes and the maximum order of EPD that can be obtained is N. Referring to the case in Fig. 2 with four microstrip lines over a grounded dielectric substrate satisfying reflection symmetry, the highest order of EPD that can be obtained is four. In order to have a DBE when only two coupled microstrips are used, reflection (mirror) symmetry must be broken, and this has been shown in [11].

When coupled waveguides with an odd number of modes N (in each direction) are considered, referring to Fig. 3 we write the state vector as  $\mathbf{\Psi} = \begin{bmatrix} \mathbf{\Psi}_U^T, & \mathbf{\Psi}_0^T, & \mathbf{\Psi}_L^T \end{bmatrix}^T$ , where the subscript 0 refers to the mode guided by the central microstrip in Fig. 3. We assume that the central microstrip supports only a single mode in each direction characterized by  $\mathbf{\Psi}_0$ , which is a two-dimensional column vector. Following the same formulation mentioned above one can prove that the transfer matrix  $\mathbf{T}_X$  for odd number of modes N reads as

$$\underline{\mathbf{T}}_{X} = \begin{bmatrix}
\underline{\mathbf{T}}_{UU}(z) + \underline{\mathbf{T}}_{LU}(z) & \underline{\mathbf{T}}_{U0}(z) + \underline{\mathbf{T}}_{L0}(z) & \mathbf{0} \\
\underline{\mathbf{T}}_{0U}(z) & \underline{\mathbf{T}}_{00}(z) & \mathbf{0} \\
\mathbf{0} & \mathbf{0} & \underline{\mathbf{T}}_{LL}(z) - \underline{\mathbf{T}}_{LU}(z)
\end{bmatrix} + 0.5(\mathbf{I} + \mathbf{R})(\mathbf{T} - \mathbf{R} \mathbf{T} \mathbf{R}) \mathbf{R}.$$
(8)

From this equation we conclude that for guiding structures with reflection symmetry, where  $\mathbf{R}\mathbf{T}\mathbf{R} - \mathbf{T} = \mathbf{0}$ , the maximum order of EPD that may be obtained is N+1 and that an EPD of order N cannot be obtained due to reciprocity. The waveguide in Fig. 3(a) is an example of this case which has reflection (mirror) symmetry so that it may

only exhibit 2<sup>nd</sup> and 4<sup>th</sup> order EPDs but can never exhibit 3<sup>rd</sup> order EPD.

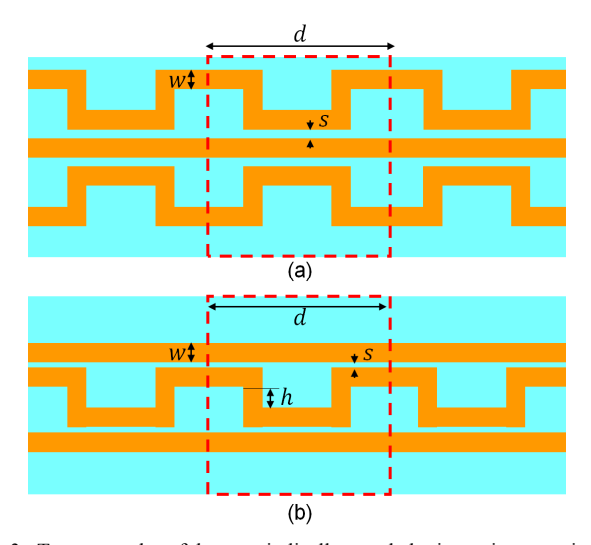


Fig. 3. Two examples of three periodically coupled microstrip transmission lines. (a) Structure with reflection symmetry that can never exhibit a SIP (a 3<sup>rd</sup> order EPD). (b) Structure with higher symmetry (glide symmetry) exhibiting a SIP.

For glide symmetric waveguides, it is obvious that  $\underline{T} \neq \underline{RTR}$  for the cases of even and odd N because  $\underline{R}$  and  $\underline{T}$  do not commute in this case, and they only commute if and only if the waveguide has reflection symmetry. This implies that when N is either even or odd, we have coupling between even and odd waveguide modes which is a necessary but not sufficient condition to achieve full degeneracy (degeneracy of order 2N).

We consider now a numerical example of three coupled microstrip transmission lines as shown in Fig. 3(b) which was presented in [17]. For simplicity we assume that the structure is lossless. The microstrip waveguide in Fig. 3(b) is glide symmetric and does not prohibit the coupling between all the waveguide modes and therefore it may also exhibit a  $3^{rd}$  order EPD. Indeed, Fig. 4 shows the dispersion relation for propagating modes (i.e., with wavenumbers with vanishing imaginary part) in the waveguide in Fig. 3(b) after engineering it to exhibit an SIP (a  $3^{rd}$  order EPD) at frequency f=2 GHz. The used parameters are (in mm) w=3, s=0.5,

h = 29.3, and d = 76.8. The microstrips are above a grounded dielectric substrate with relative dielectric constant of 6.15 and height of 1.52 mm.

This proves that introducing higher symmetries in a waveguide allows the existence of new EPDs that cannot be obtained under simpler waveguides that satisfy mirror symmetry.

# III. CONCLUSION

Symmetry plays an important role in the existence of higher order EPDs. Reflection symmetry prohibits the existence of degenerate band edge (DBE) in two coupled periodic waveguides. Reflection symmetry must be broken for two coupled waveguides to support a DBE.

Reflection symmetry also prohibits the existence of stationary inflection point (SIP) in three coupled periodic waveguides. Glide symmetry enables the possibility for the SIP to exist in three coupled waveguides.

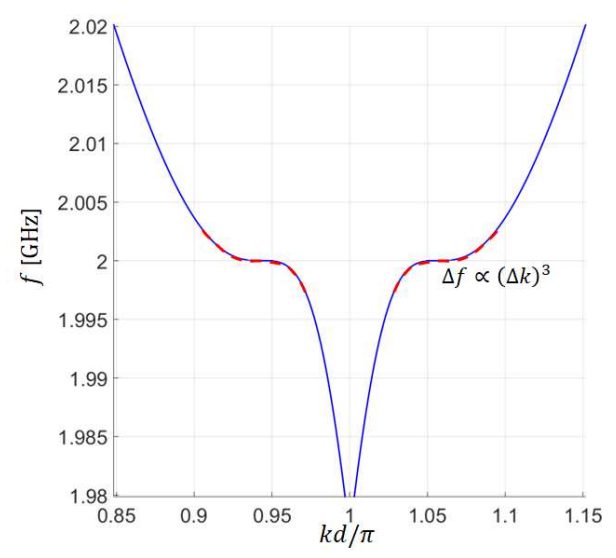


Fig. 4. Wavenumber dispersion diagram for a mode in the waveguide with glide symmetry in Fig. 3(b), showing the existence of a SIP, which is a third order EPD, at f=2 GHz. Here, we plot only the two modes with purely real wavenumber. Each mode exhibits an SIP (or frozen mode). This plot does not show the coalescence of three modes at each SIP because the other two coalescing modes have complex wavenumber, hence not shown here.

### ACKNOWLEDGMENT

This material is based on work supported by the Air Force Office of Scientific Research award number FA9550-18-1-0355, and by the National Science Foundation under award NSF ECCS-1711975.

# REFERENCES

- [1] A. Figotin and I. Vitebskiy, "Oblique frozen modes in periodic layered media," *Phys. Rev. E*, vol. 68, no. 3, Sep. 2003, Art. no. 036609.
- [2] A. Figotin and I. Vitebskiy, "Frozen light in photonic crystals with degenerate band edge," *Phys. Rev. E*, vol. 74, no. 6, Dec. 2006, Art. no. 066613.
- [3] Tarek Mealy, Ahmed F Abdelshafy, and Filippo Capolino, "The Degeneracy of the Dominant Mode in Rectangular Waveguide", in 2019 United States National Committee of URSI National Radio Science Meeting (USNC-URSI NRSM), Boulder, CO, USA, Jan. 2019.
- [4] R. El-Ganainy, K. G. Makris, D. N. Christodoulides, and Z. H. Musslimani, "Theory of coupled optical *PT*-symmetric structures," *Opt. Lett.*, vol. 32, no. 17, pp. 2632–2634, Aug. 2007.
- [5] S. Bittner et al., "PT symmetry and spontaneous symmetry breaking in a microwave billiard," Phys. Rev. Lett., vol. 108, Jan. 2012, Art. no. 024101
- [6] M. A. Othman and F. Capolino, "Theory of exceptional points of degeneracy in uniform coupled waveguides and balance of gain and loss," *IEEE Trans. Antennas Propag.*, vol. 65, no. 10, pp. 5289–5302, Aug. 2017.

- [7] C. Locker, K. Sertel, and J. L. Volakis, "Emulation of propagation in layered anisotropic media with equivalent coupled microstrip lines," *IEEE Microw. Wireless Compon. Lett.*, vol. 16, no. 12, pp. 642–644, Dec. 2006.
- [8] J. R. Burr, N. Gutman, C. M. de Sterke, I. Vitebskiy, and R. M. Reano, "Degenerate band edge resonances in coupled periodic silicon optical waveguides," *Optics Express*, vol. 21, no. 7, pp. 8736–8745, Apr. 2013
- [9] M. A. Othman and F. Capolino, "Demonstration of a degenerate band edge in periodically-loaded circular waveguides," *IEEE Microw. Wireless Compon. Lett.*, vol. 25, no. 11, pp. 700–702, Oct. 2015.
- [10] M. Y. Nada, M. A. Othman, and F. Capolino, "Theory of coupled resonator optical waveguides exhibiting high-order exceptional points of degeneracy," *Phy. Rev. B*, vol. 96, no. 18, Nov. 2017, Art. no. 184304.
- [11] A. F. Abdelshafy, M. A. Othman, D. Oshmarin, A. T. Almutawa, and F. Capolino, "Exceptional Points of Degeneracy in Periodic Coupled Waveguides and the Interplay of Gain and Radiation Loss: Theoretical and Experimental Demonstration," *IEEE Trans. Antennas Propag.*, vol. 67, no. 11, pp. 6909–6923, Nov. 2019.
- [12] M. B. Stephanson, K. Sertel and J. L. Volakis, "Frozen Modes in Coupled Microstrip Lines Printed on Ferromagnetic Substrates," *IEEE Microw. Wireless Compon. Lett.*, vol. 18, no. 5, pp. 305–307, May 2008
- [13] G. Mumcu, K. Sertel and J. L. Volakis, "Lumped Circuit Models for Degenerate Band Edge and Magnetic Photonic Crystals," *IEEE Microw. Wireless Compon. Lett.*, vol. 20, no. 1, pp. 4–6, Jan. 2010.
- [14] A. Hessel, Ming Hui Chen, R. C. M. Li and A. A. Oliner, "Propagation in periodically loaded waveguides with higher symmetries," *Proc. of the IEEE*, vol. 61, no. 2, pp. 183–195, Feb. 1973.
- [15] M. Bagheriasl, O. Quevedo-Teruel and G. Valerio, "Bloch Analysis of Artificial Lines and Surfaces Exhibiting Glide Symmetry," in *IEEE Trans. Microw. Theory Techn.*, vol. 67, no. 7, pp. 2618–2628, Jul. 2019.
- [16] F. Ghasemifard, M. Norgren, O. Quevedo-Teruel, and G. Valerio, "Analyzing glide-symmetric holey metasurfaces using a generalized floquet theorem," *IEEE Access*, vol. 6, pp. 71743–71750, Nov. 2018.
- [17] M. Y. Nada, T. Mealy, and F. Capolino, "Frozen Mode in Three-Way Periodic Microstrip Coupled Waveguide," *IEEE Microw. Wireless Compon. Lett.*, vol. 31, no. 3, pp. 229–232, Mar. 2020.